

Search for Rare Decays of D^0 Mesons into Two Muons

R. Aaij *et al.*^{*}
(LHCb Collaboration)



(Received 21 December 2022; accepted 18 May 2023; published 26 July 2023)

A search for the very rare $D^0 \rightarrow \mu^+ \mu^-$ decay is performed using data collected by the LHCb experiment in proton-proton collisions at $\sqrt{s} = 7, 8$, and 13 TeV, corresponding to an integrated luminosity of 9 fb^{-1} . The search is optimized for D^0 mesons from $D^{*+} \rightarrow D^0 \pi^+$ decays but is also sensitive to D^0 mesons from other sources. No evidence for an excess of events over the expected background is observed. An upper limit on the branching fraction of this decay is set at $\mathcal{B}(D^0 \rightarrow \mu^+ \mu^-) < 3.1 \times 10^{-9}$ at a 90% C.L. This represents the world's most stringent limit, constraining models of physics beyond the standard model.

DOI: 10.1103/PhysRevLett.131.041804

Processes with a change in quark flavor without a change in electric charge are forbidden at the lowest order in the standard model (SM) of particle physics. Flavor changing neutral currents (FCNC) are additionally suppressed by the Glashow-Iliopoulos-Maiani (GIM) mechanism [1]. FCNC have been extensively studied in strange- and beauty-quark hadrons. In the charm sector the GIM suppression is stronger because the mass differences between down-type quarks are smaller than the ones between up-type quarks. These processes can be enhanced by several orders of magnitude in new physics (NP) scenarios when compared with the SM.

The $D^0 \rightarrow \mu^+ \mu^-$ decay is among the most interesting charm-hadrons decays (Charge conjugate processes are implied throughout.), being fully leptonic and additionally suppressed by helicity reasons. Its SM short-distance contribution is extremely suppressed, yielding a branching fraction on the order of 10^{-18} [2]. Long-distance contributions dominate through an intermediate two-photon state, and can be estimated to be $\mathcal{B}(D^0 \rightarrow \mu^+ \mu^-) \simeq 2.7 \times 10^{-5} \mathcal{B}(D^0 \rightarrow \gamma\gamma)$, leading to a $D^0 \rightarrow \mu^+ \mu^-$ branching fraction of at least 3×10^{-13} [2]. The best upper limit on the $D^0 \rightarrow \gamma\gamma$ decay rate was set by the Belle Collaboration to be 8.5×10^{-7} at a 90% C.L. [3]; using the same relation this turns into an upper limit on the long-distance contribution to the $D^0 \rightarrow \mu^+ \mu^-$ branching fraction of 2.3×10^{-11} . The $D^0 \rightarrow \mu^+ \mu^-$ decay rate can be enhanced in many NP models [4]. Being one of the most sensitive FCNC processes in the up-quark sector, its branching fraction is used as a primary building block of different

models, constraining the relevant couplings saturating the branching fraction limit [5–16]. Most significantly, model-independent bounds on the Wilson coefficients related to charm physics and in particular to $D^0 \rightarrow \mu^+ \mu^-$ decays have been set in Refs. [16,17]. Furthermore, the $D^0 \rightarrow \mu^+ \mu^-$ rate is correlated to the rate of $D^0 - \bar{D}^0$ mixing in many NP models [4]. This is of utmost importance given the recent first observation of the mass difference between neutral charm-meson eigenstates [18]. Concerning specific models, in the minimal supersymmetric standard model no sizeable contribution would enhance the $D^0 \rightarrow \mu^+ \mu^-$ rate [4]. Conversely, in some supersymmetric models with R -parity symmetry violation tree level contributions would be allowed [2,19]. Recent discussions of predictions for $D^0 \rightarrow \mu^+ \mu^-$ decays in such models can be found in Refs. [14,20]. In addition, it is interesting to note the importance of $D^0 \rightarrow \mu^+ \mu^-$ decays as a testing ground for models with leptoquarks proposed to explain deviations from the SM observed in B physics measurements [21–40]. In some of these models rare B decays receive contributions at the loop level, while new particles could mediate the $D^0 \rightarrow \mu^+ \mu^-$ decay at tree level. This phenomenon has been extensively discussed in the literature [5–13,41–46]. In those where additional vector bosons (Z') are introduced, the $D^0 \rightarrow \mu^+ \mu^-$ decay usually does not give strong constraints [47,48]. Similarly, in other explanatory models [49–51] the bound from $D^0 \rightarrow \mu^+ \mu^-$ decays can be avoided. Instead in some models with vectorlike fermions [15], the $D^0 \rightarrow \mu^+ \mu^-$ decay gives the strongest constraint.

The current world's best limit on this decay is $\mathcal{B}(D^0 \rightarrow \mu^+ \mu^-) < 6.2 \times 10^{-9}$ (7.6×10^{-9}) at 90% (95%) C.L., and was obtained by the LHCb experiment exploiting about 0.9 fb^{-1} of 2011 data [52]. The data used in Ref. [52] are also used in this analysis, and those results are superseded by this Letter.

This Letter presents a search for the $D^0 \rightarrow \mu^+ \mu^-$ decay based on data collected by the LHCb experiment

^{*}Full author list given at the end of the article.

in pp collisions corresponding to 9 fb^{-1} of integrated luminosity. The data have been collected in 2011, 2012 (Run 1), and 2015–2018 (Run 2) at $\sqrt{s} = 7, 8, \text{ and } 13 \text{ TeV}$, respectively. Compared with the previous publication [52], the present work benefits from various improvements in the analysis, such as refined multivariate algorithms against combinatorial and misidentified background as well as an improved trigger [53], described throughout the Letter. These allow one to mitigate the impact of the harsher experimental conditions in Run 2. Both the higher energy and instantaneous luminosity produce a higher track multiplicity, which increases the combinatorial background and worsens the particle identification performance. The $D^0 \rightarrow \mu^+ \mu^-$ decay is searched for using $D^{*+} \rightarrow D^0 \pi^+$ decays, as this improves the background rejection and allows the yield of the decay to be obtained from a two-dimensional fit to the dimuon invariant mass, $m(\mu^+ \mu^-)$, and the difference between the D^{*+} and D^0 candidate masses, Δm . The yield is converted to the decay branching fraction by normalizing to two hadronic decays, $D^0 \rightarrow K^- \pi^+$ and $D^0 \rightarrow \pi^+ \pi^-$, selected concurrently to the signal (collectively referred to as $D^0 \rightarrow h^+ h^-$).

The LHCb detector is a single-arm forward spectrometer covering the pseudorapidity range $2 < \eta < 5$, described in detail in Refs. [54,55]. The simulated events used in this analysis are produced with the software described in Refs. [56–62].

Events are selected online by a trigger that consists of a hardware stage, which is based on information from the calorimeter and muon systems, followed by two software stages. At the hardware trigger stage, events are required to have a muon candidate with high transverse momentum, p_T , or a hadron, photon or electron candidate with high transverse energy in the calorimeters. A first stage of the software trigger selects events with a muon candidate, or a high p_T charged particle, or a combination of two tracks, each of these displaced from the primary pp collision vertex (PV). In the second stage of the software trigger, dedicated algorithms select candidate $D^0 \rightarrow \mu^+ \mu^-$, $D^0 \rightarrow K^- \pi^+$ and $D^0 \rightarrow \pi^+ \pi^-$ decays, combining two oppositely charged tracks with loose particle identification (PID) requirements that form a secondary vertex separated from any PV. The invariant mass of the D^0 candidate must lie in an interval of $\pm 300(\pm 70) \text{ MeV}/c^2$ centered on the known D^0 mass for signal (normalization) channel candidates. To keep the same trigger selection for the signal and normalization channels, aside from PID, a scale factor of order 0.2–3.0% depending on the data taking period is applied to the normalization channels' trigger selections to limit their rate, keeping randomly a fraction of the events. In the offline selection, only candidates associated with a muon hardware trigger, or those where the rest of the event contained a high transverse energy hadron or electron are kept for the signal channel. For the normalization channels, only candidates associated with a high transverse energy hadron are kept.

In the offline analysis, D^0 candidates satisfying the trigger requirements are formed with similar but more stringent criteria than the second software-trigger stage. These D^0 candidates are then combined with a charged particle originating from the same PV and having $p_T > 110 \text{ MeV}/c$ to form $D^{*+} \rightarrow D^0 \pi^+$ candidates. To improve the mass resolution, the D^{*+} meson decay vertex is constrained to coincide with the PV [63]. The candidate Δm is required to be in the range $139.6\text{--}151.6 \text{ MeV}/c^2$. A multivariate selection based on a boosted decision tree (BDT) algorithm [64–66] is used to suppress background from random combinations of charged particles, using as input the p_T of the pion from the D^{*+} decay, the smallest p_T and impact parameter significance with respect to the PV of the D^0 decay products, the angle between the D^0 momentum and the vector connecting the primary and secondary vertices, and the quality of the D^0 vertex. The BDT is trained separately for each Run of data taking, using simulated decays as signal and data candidates from the dimuon sample with $m(\mu^+ \mu^-) > 1894 \text{ MeV}/c^2$ as background. The k -folding technique, with $k = 9$, is applied [67]. The BDT output ranges from 0 to 1, from backgroundlike candidates to more signal-like candidates. The BDT output is used to define three search regions: $\text{BDT} \in [0.15, 0.33]$, $[0.33, 0.66]$, $[0.66, 1.0]$. The output of the same BDT algorithm is computed also for the $D^0 \rightarrow \pi^+ \pi^-$ candidates for calibration purposes, but is not required in the selection.

A second source of background is due to two- and three-body D^0 decays, with one or two hadrons misidentified as muons (e.g., $D^0 \rightarrow h^+ h^-$ or semileptonic decays). The misidentification occurs mainly for hadrons that decay into a muon before the muon subdetector. Although this process is relatively rare, the large branching fractions of these modes produce a background peaking in the signal region of the $m(\mu^+ \mu^-)$ distribution that is partially suppressed by a multivariate muon identification discriminant combining information from the Cherenkov detectors, the calorimeters, and the muon subdetector [68]. In addition, the muon candidates are required to have associated muon chamber hits that are not shared with any other track in the event. Signal and background sources can originate both from $D^{*+} \rightarrow D^0 \pi^+$ decays or from other sources (the PV or B decays) combined with an unrelated pion (untagged); both are taken into account in the yield estimation. A requirement on the output of the multivariate muon identification discriminant is simultaneously chosen for the three BDT regions, by optimizing the sensitivity to the minimum visible cross section, as defined by an extension of the figure of merit defined in Ref. [69]. Roughly 1% of events contain more than one signal candidate after all selection requirements, all of which are retained.

The signal yield is converted to the decay branching fraction by normalizing to the hadronic decays $D^0 \rightarrow \pi^+ \pi^-$

and $D^0 \rightarrow K^-\pi^+$, with branching fractions of $(1.490 \pm 0.027) \times 10^{-3}$ and $(3.999 \pm 0.045) \times 10^{-2}$, respectively [70], as

$$\begin{aligned} \mathcal{B}(D^0 \rightarrow \mu^+\mu^-) &= \frac{N_{D^0 \rightarrow \mu^+\mu^-}}{N_{D^0 \rightarrow h^+h^-}} \frac{\epsilon_{h^+h^-}}{\epsilon_{\mu^+\mu^-}} s \mathcal{B}(D^0 \rightarrow h^+h^-) \\ &\equiv \alpha N_{D^0 \rightarrow \mu^+\mu^-} \end{aligned} \quad (1)$$

where ϵ is the efficiency and N is the yield of the given channel, s is the scale factor of the normalization channel and α is defined as the single event sensitivity.

The efficiencies in Eq. (1) are factorized into different steps for ease of estimation and evaluated with respect to the previous steps: detector acceptance, reconstruction and selection, PID, and trigger.

The reconstruction and selection efficiencies are obtained from simulated samples. The simulated candidates are assigned weights with an iterative procedure that improves the agreement with data using the following variables: pseudorapidity of the D^0 meson, transverse momentum of the D^0 meson, and number of tracks in the event. It is verified that after weighting, all variables used in the selection agree well between data and simulation. The weights obtained from the $D^0 \rightarrow \pi^+\pi^-$ candidates are used to correct also the signal simulation.

Possible residual differences between data and simulation in the tracking efficiencies are determined using control channels in data [71]. The PID efficiencies are determined from data using samples of kinematically identified charged particles from $B^+ \rightarrow J/\psi K^+$ and $D^{*+} \rightarrow D^0(\rightarrow K^-\pi^+)\pi^+$ decays [68], weighted to match the kinematic properties of the signal and the normalization channels, respectively. The efficiencies are determined in bins of the p and p_T of the tracks. A total systematic uncertainty of 1–3% is associated to the binning scheme and background determination in the calibration samples.

The efficiency of the second level of the software trigger is unity with respect to the offline-selected candidates by construction, as the selection is tighter in every requirement. The hardware and first level software trigger efficiencies are evaluated with the TISTOS method [72] in data. For the signal channel, the $B^+ \rightarrow J/\psi(\rightarrow \mu^+\mu^-)K^+$ decay is used as the calibration channel, selected with the same requirements as those used for the analysis of B decays into two muons [73,74]. The calibration is performed in intervals of the $J/\psi p_T$ and pseudorapidity. For each interval, a scaling factor between data and simulation is obtained and applied to the $D^0 \rightarrow \mu^+\mu^-$ simulation. Compatible results are obtained repeating the calibration in intervals of p_T and the maximum $\text{IP}\chi^2$ of the muons, where $\text{IP}\chi^2$ is defined as the difference in the vertex-fit χ^2 of a given PV reconstructed with and without the track under consideration. The typical scaling between data and simulation deviates from unity by 2–6%. The normalization

channels, given their high yields, are self-calibrated. The TISTOS method is applied to the $D^0 \rightarrow K^-\pi^+$ and $D^0 \rightarrow \pi^+\pi^-$ channels, and trigger efficiencies are obtained. To minimize cross-correlation biases, only candidates in events that satisfy a muon trigger independently of the candidate are used as a calibration sample. The calibration of the hadronic hardware trigger is also validated with independent estimates based on control samples in data, obtained with similar methods as in Ref. [75], from which a 15% relative systematic uncertainty is assigned to the hadronic trigger efficiency calibration.

The efficiency of the BDT requirement, and the signal fraction in the BDT intervals, are calibrated in data by applying the same estimator to the $D^0 \rightarrow \pi^+\pi^-$ decay, which is topologically very similar to the signal. The distribution of the BDT output is obtained in background subtracted $D^0 \rightarrow \pi^+\pi^-$ decays in data and simulation, and found to be compatible, as shown in the Supplemental Material [76]. A small correction is determined and applied to the signal; its uncertainty is assigned as systematic uncertainty to the signal efficiency.

The yields of the normalization channels are obtained through a fit to the Δm distribution (Fig. 1), requiring the reconstructed D^0 mass to be within $\pm 10 \text{ MeV}/c^2$ of the known D^0 mass. The signal probability distribution function is composed of a sum of a Gaussian and a Crystal-Ball function [77] with power-law tails on both sides. The background is described with a threshold function, as defined in Ref. [52]. The parameters of the Crystal-Ball function are estimated with simulation: the power of the tail is fixed, while the position where the power tails start may vary freely in the fit. In addition, the signal width and all background parameters are left free in the fit.

Using Eq. (1), values of α for both normalization channels are obtained, and found to be in good agreement with each other for each data taking run and for the full sample. As an additional cross-check, the ratio of the efficiency corrected yields of the two normalization channels is obtained and compared to the ratio of their branching fractions. The value is stable across the data taking years and compatible with the world average [70]. The average single event sensitivity is found to be $\alpha = (2.15 \pm 0.34) \times 10^{-11}$, corresponding to at most one expected signal $D^0 \rightarrow \mu^+\mu^-$ decay under the SM hypothesis.

The signal yield is obtained through an unbinned maximum-likelihood fit to the two-dimensional distribution of $m(\mu^+\mu^-)$ and Δm , performed simultaneously in the three BDT intervals and in the two data taking Runs. The distributions projected onto the two variables are shown in Fig. 2. Each of the two projections is selected using only candidates in the signal region of the other variable, where the signal regions are defined as $m(D^0) \in [1840, 1885] \text{ MeV}/c^2$ and $\Delta m \in [144.9, 146.1] \text{ MeV}/c^2$, respectively. The full distributions can be seen in the

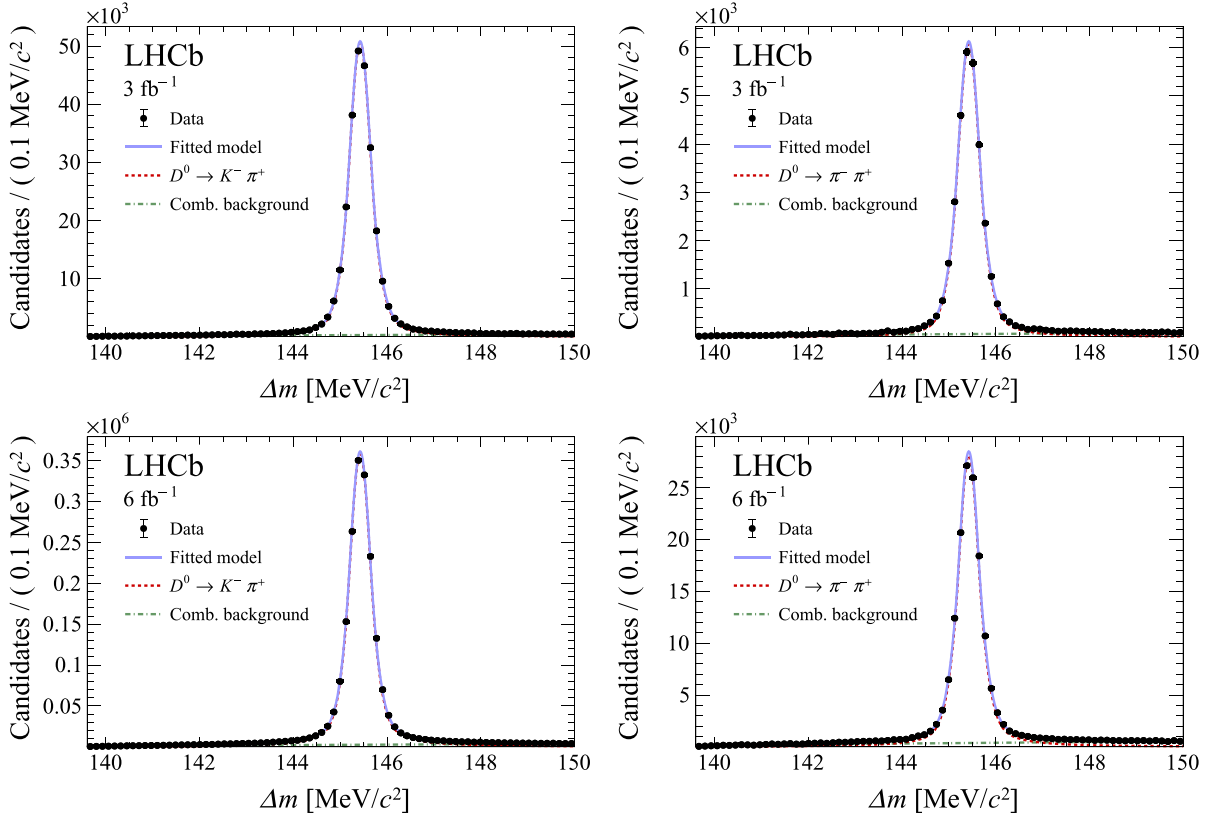


FIG. 1. Distributions of Δm for (left) $D^0 \rightarrow K^-\pi^+$ and (right) $D^0 \rightarrow \pi^+\pi^-$ normalization channel candidates for (top) Run 1 and (bottom) Run 2 data. The distributions are superimposed with the fit.

Supplemental Material [76]. The correlation between the two variables is found to be negligible for all contributing decay modes; thus they are treated as uncorrelated. After the full selection, only combinatorial and misidentified hadronic D^0 decays are found to contribute to the background. Background from semileptonic decays is found to be negligible, and any remaining background from other sources is well modeled as part of the combinatorial background component.

The shape of the signal and misidentified background ($D^0 \rightarrow \pi^+\pi^-$, $D^0 \rightarrow K^-\pi^+$) distributions in the two fit variables is obtained from simulation, reconstructed as $D^0 \rightarrow \mu^+\mu^-$ decays. The model parameters are determined separately for Run 1 and Run 2; the resulting probability distribution function describes the distribution in each data taking year and BDT interval well. For signal, the $m(\mu^+\mu^-)$ and Δm distributions are both parametrized by Crystal-Ball [77] functions with power tails on both sides. For $D^0 \rightarrow \pi^+\pi^-$ decays, a single Crystal-Ball function in $m(\mu^+\mu^-)$ and the sum of a Johnson [78] and Gaussian function in Δm are employed. For $D^0 \rightarrow K^-\pi^+$ decays, a Johnson function is used for the $m(\mu^+\mu^-)$ distribution, while the Δm distribution is described by three Gaussian functions. The combinatorial background is described by an exponential function in $m(\mu^+\mu^-)$ and a threshold function in Δm [52].

Untagged signal and $D^0 \rightarrow \pi^+\pi^-$ components are included and parametrized as their respective tagged component in $m(\mu^+\mu^-)$ and with the same threshold function of the combinatorial background in Δm . The fraction of this component is fixed to the value determined in each BDT interval from a fit to $D^0 \rightarrow \pi^+\pi^-$ data. The shape parameters obtained from the simulated samples are fixed in the data fit, while the slope of the exponential of the combinatorial background is left free to vary in each BDT interval.

A constraint on the expected number of misidentified $D^0 \rightarrow \pi^+\pi^-$ decays is determined from a dedicated, high-statistics, simulation sample with the trigger and offline selection applied. The most critical part of the simulated sample is the PID efficiency due to the presence of a large fraction of $\pi \rightarrow \mu$ decays that mimic the signal and are not considered in the standard calibration tools. The PID efficiency is obtained from simulation, but it is cross-checked using $D^+ \rightarrow \pi^+\pi^-\pi^+$ and $D_s^+ \rightarrow \pi^+\pi^-\pi^+$ control samples in data where same-sign pions are weighted to match the kinematics of $D^0 \rightarrow \pi^+\pi^-$ decays. The agreement between the PID efficiency determined with both methods is satisfactory over the full range of the muon identification discriminant variable [76]. Therefore, no systematic uncertainty is assigned on this estimate. The uncertainty on the expected $D^0 \rightarrow \pi^+\pi^-$ yield is

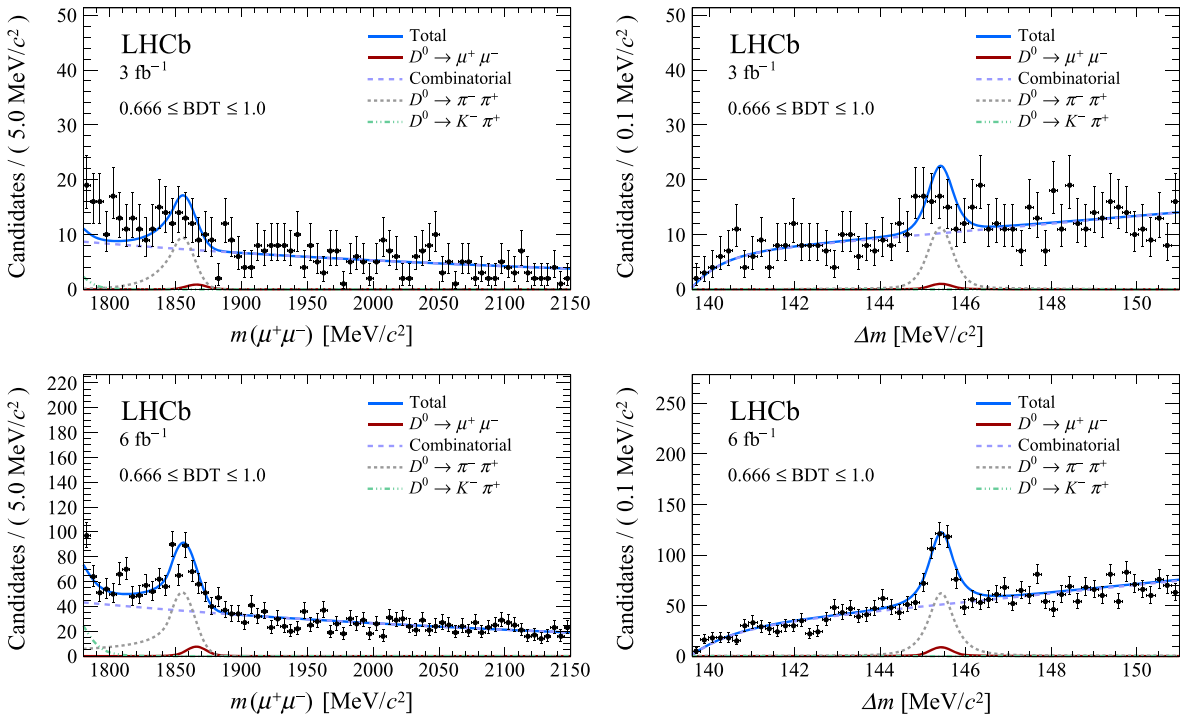


FIG. 2. Distribution of (left) $m(\mu^+\mu^-)$ and (right) Δm for the $D^0 \rightarrow \mu^+\mu^-$ candidates in data from (top) Run 1 and (bottom) Run 2, for the most sensitive BDT interval. The distribution is superimposed with the fit to data. Each of the two distributions is in the signal region of the other variable; see text for details. Untagged and tagged decays are included in a single component for signal and $D^0 \rightarrow \pi^+\pi^-$ background.

propagated through a Gaussian constraint on the relevant parameter in the final fit.

The yield of the misidentified $D^0 \rightarrow K^-\pi^+$ decays is constrained from an auxiliary fit to the $m(\mu^+\mu^-)$ sideband data, recomputed with the correct mass hypothesis. The fit is performed using the Δm distribution within a ± 10 MeV/ c^2 region around the D^0 mass in the $K^-\pi^+$ mass hypothesis. A correction is applied to take into account this mass requirement. The correlation between this estimate and the yield in the final fit is found not to influence the estimate of the signal branching fraction.

The systematic uncertainties related to both the normalization, through α , and the background shapes and yields, are included in the fit as Gaussian constraints on the relevant parameters. The dominant systematic uncertainty comes from the calibration of the hadronic trigger efficiency, which is shared through auxiliary parameters among the normalization channels, and also with the misidentified $D^0 \rightarrow \pi^+\pi^-$ yields that depend on the same estimate. The fit procedure is tested with pseudoexperiments. The values of the floating shape parameters are obtained from the data fit. Unbiased estimates of the branching fraction with correct coverage are obtained.

The $m(\mu^+\mu^-)$ and Δm distributions in data are shown for the most sensitive BDT interval in Fig. 2 and for all intervals in Ref. [76], overlaid with the result of the fit. The data are consistent with the expected background. The

value obtained for the $D^0 \rightarrow \mu^+\mu^-$ branching fraction is $\mathcal{B}(D^0 \rightarrow \mu^+\mu^-) = (1.7 \pm 1.0) \times 10^{-9}$, corresponding to 79 ± 45 signal decays. The significance of this signal is estimated comparing the test statistics in data with the distribution of the test statistics in background-only pseudoexperiments, and is found to have a p value of 0.068, corresponding to a significance of 1.5σ (see also Ref. [76]). An upper limit on the branching fraction is derived using the frequentist C.L._s method [79] as implemented in the GAMMACOMBO framework [80,81]. This yields

$$\mathcal{B}(D^0 \rightarrow \mu^+\mu^-) < 3.1(3.5) \times 10^{-9} \text{ at } 90(95)\% \text{C.L.}$$

The observed limit is larger than the one expected from background-only pseudoexperiments, $\mathcal{B}(D^0 \rightarrow \mu^+\mu^-) < 1.9(2.3) \times 10^{-9}$ at a 90(95%) C.L., coherently with the central value for the signal branching fraction.

The fit is repeated with different configurations: allowing the resolution of the misidentified $D^0 \rightarrow \pi^+\pi^-$ background to vary, using a double exponential function in place of a single one for the combinatorial background, and reducing the range in the Δm variable. No significant change was found in the signal branching fraction with any configuration.

In summary, a search for the $D^0 \rightarrow \mu^+\mu^-$ decay in data corresponding to 9 fb^{-1} of pp collision data collected by the LHCb experiment is performed. No excess with respect

to the background expectation has been found, and an upper limit of $\mathcal{B}(D^0 \rightarrow \mu^+ \mu^-) < 3.1 \times 10^{-9}$ at 90% C.L. has been set. This result represents an improvement of more than a factor of 2 with respect to the previous LHCb result. This measurement constitutes the most stringent limit on the relevant FCNC couplings in the charm sector, allowing one to set additional constraints on physics models beyond the SM which predict the branching fractions of $D^0 \rightarrow \mu^+ \mu^-$ and describe results from B physics measurements.

We express our gratitude to our colleagues in the CERN accelerator departments for the excellent performance of the LHC. We thank the technical and administrative staff at the LHCb institutes. We acknowledge support from CERN and from the national agencies: CAPES, CNPq, FAPERJ, and FINEP (Brazil); MOST and NSFC (China); CNRS/IN2P3 (France); BMBF, DFG, and MPG (Germany); INFN (Italy); NWO (Netherlands); MNiSW and NCN (Poland); MEN/IFA (Romania); MICINN (Spain); SNSF and SER (Switzerland); NASU (Ukraine); STFC (United Kingdom); DOE NP and NSF (USA). We acknowledge the computing resources that are provided by CERN, IN2P3 (France), KIT and DESY (Germany), INFN (Italy), SURF (Netherlands), PIC (Spain), GridPP (United Kingdom), CSCS (Switzerland), IFIN-HH (Romania), CBPF (Brazil), Polish WLCG (Poland), and NERSC (USA). We are indebted to the communities behind the multiple open-source software packages on which we depend. Individual groups or members have received support from ARC and ARDC (Australia); Minciencias (Colombia); AvH Foundation (Germany); EPLANET, Marie Skłodowska-Curie Actions, and ERC (European Union); A*MIDEX, ANR, IPhU and Labex P2IO, and Région Auvergne-Rhône-Alpes (France); Key Research Program of Frontier Sciences of CAS, CAS PIFI, CAS CCEPP, Fundamental Research Funds for the Central Universities, and Sci. & Tech. Program of Guangzhou (China); GVA, XuntaGal, GENCAT, and Prog. Atracción Talento, CM (Spain); SRC (Sweden); the Leverhulme Trust, the Royal Society, and UKRI (United Kingdom).

- [1] S. L. Glashow, J. Iliopoulos, and L. Maiani, Weak interactions with lepton-hadron symmetry, *Phys. Rev. D* **2**, 1285 (1970).
- [2] G. Burdman, E. Golowich, J. L. Hewett, and S. Pakvasa, Rare charm decays in the Standard Model and beyond, *Phys. Rev. D* **66**, 014009 (2002).
- [3] N. K. Nisar *et al.* (Belle Collaboration), Search for the rare decay $D^0 \rightarrow \gamma\gamma$ at Belle, *Phys. Rev. D* **93**, 051102 (2016).
- [4] E. Golowich, J. A. Hewett, S. Pakvasa, and A. A. Petrov, Relating $D^0 - \bar{D}^0$ mixing and $D^0 \rightarrow l^+ l^-$ with new physics, *Phys. Rev. D* **79**, 114030 (2009).
- [5] M. Bauer and M. Neubert, Minimal Leptoquark Explanation for the $R_{D^{(*)}}$, R_K , and $(g-2)_g$ Anomalies, *Phys. Rev. Lett.* **116**, 141802 (2016).

- [6] S. Fajfer and N. Košnik, Leptoquarks in flavor changing neutral current charm decays, *Phys. Rev. D* **79**, 017502 (2009).
- [7] D. Bećirević, N. Košnik, O. Sumensari, and R. Zukanovich Funchal, Palatable leptoquark scenarios for lepton flavor violation in exclusive $b \rightarrow s\ell_1\ell_2$ modes, *J. High Energy Phys.* **11** (2016) 035.
- [8] Y. Cai, J. Gargalionis, M. A. Schmidt, and R. R. Volkas, Reconsidering the one leptoquark solution: Flavor anomalies and neutrino mass, *J. High Energy Phys.* **10** (2017) 047.
- [9] K. Kowalska, E. M. Sessolo, and Y. Yamamoto, Constraints on charmphilic solutions to the muon g-2 with leptoquarks, *Phys. Rev. D* **99**, 055007 (2019).
- [10] I. Bigaran, J. Gargalionis, and R. R. Volkas, A near-minimal leptoquark model for reconciling flavor anomalies and generating radiative neutrino masses, *J. High Energy Phys.* **10** (2019) 106.
- [11] I. Doršner, S. Fajfer, and O. Sumensari, Muon $g-2$ and scalar leptoquark mixing, *J. High Energy Phys.* **06** (2020) 089.
- [12] K. Kowalska, E. M. Sessolo, and Y. Yamamoto, Flavor anomalies from asymptotically safe gravity, *Eur. Phys. J. C* **81**, 272 (2021).
- [13] M. Bordone, O. Catà, T. Feldmann, and R. Mandal, Constraining flavour patterns of scalar leptoquarks in the effective field theory, *J. High Energy Phys.* **03** (2021) 122.
- [14] W. Altmannshofer, P. S. B. Dev, A. Soni, and Y. Sui, Addressing $R_{D^{(*)}}$, $R_{K^{(*)}}$, muon $g-2$ and ANITA anomalies in a minimal R -parity violating supersymmetric framework, *Phys. Rev. D* **102**, 015031 (2020).
- [15] K. Ishiwata, Z. Ligeti, and M. B. Wise, New vector-like fermions and flavor physics, *J. High Energy Phys.* **10** (2015) 027.
- [16] A. Bharucha, D. Boito, and C. Méaux, Disentangling QCD and new physics in $D^+ \rightarrow \pi^+ \ell^+ \ell^-$, *J. High Energy Phys.* **04** (2021) 158.
- [17] S. Fajfer and N. Kosnik, Prospects of discovering new physics in rare charm decays, *Eur. Phys. J. C* **75**, 567 (2015).
- [18] R. Aaij *et al.* (LHCb Collaboration), Observation of the Mass Difference Between Neutral Charm-Meson Eigenstates, *Phys. Rev. Lett.* **127**, 111801 (2021).
- [19] G. Burdman and I. Shipsey, $D^0 - \bar{D}^0$ mixing and rare charm decays, *Annu. Rev. Nucl. Part. Sci.* **53**, 431 (2003).
- [20] R.-M. Wang, J.-H. Sheng, J. Zhu, Y.-Y. Fan, and Y.-G. Xu, Decays $D_{(s)}^+ \rightarrow \pi(K)^+ \ell^+ \ell^-$ and $D^0 \rightarrow \ell^+ \ell^-$ in the MSSM with and without R-parity, *Int. J. Mod. Phys. A* **30**, 1550063 (2015).
- [21] R. Aaij *et al.* (LHCb Collaboration), Test of lepton universality with $B^0 \rightarrow K^{*0} \ell^+ \ell^-$ decays, *J. High Energy Phys.* **08** (2017) 055.
- [22] R. Aaij *et al.* (LHCb Collaboration), Test of lepton universality in beauty-quark decays, *Nat. Phys.* **18**, 277 (2022).
- [23] R. Aaij *et al.* (LHCb Collaboration), Test of lepton universality using $\Lambda_b^0 \rightarrow p K^- \ell^+ \ell^-$ decays, *J. High Energy Phys.* **05** (2020) 040.
- [24] R. Aaij *et al.* (LHCb Collaboration), Angular Analysis of the $B^+ \rightarrow K^{*+} \mu^+ \mu^-$ Decay, *Phys. Rev. Lett.* **126**, 161802 (2021).

- [25] R. Aaij *et al.* (LHCb Collaboration), Measurement of CP -Averaged Observables in the $B^0 \rightarrow K^{*0}\mu^+\mu^-$ Decay, *Phys. Rev. Lett.* **125**, 011802 (2020).
- [26] R. Aaij *et al.* (LHCb Collaboration), Angular analysis of the $B^0 \rightarrow K^{*0}\mu^+\mu^-$ decay using 3 fb^{-1} of integrated luminosity, *J. High Energy Phys.* **02** (2016) 104.
- [27] R. Aaij *et al.* (LHCb Collaboration), Angular analysis of the rare decay $B_s^0 \rightarrow \phi\mu^+\mu^-$, *J. High Energy Phys.* **11** (2021) 043.
- [28] M. Aaboud *et al.* (ATLAS Collaboration), Angular analysis of $B_d^0 \rightarrow K^*\mu^+\mu^-$ decays in pp collisions at $\sqrt{s} = 8 \text{ TeV}$ with the ATLAS detector, *J. High Energy Phys.* **10** (2018) 047.
- [29] B. Aubert *et al.* (BABAR Collaboration), Measurements of branching fractions, rate asymmetries, and angular distributions in the rare decays $B \rightarrow K\ell^+\ell^-$ and $B \rightarrow K^*\ell^+\ell^-$, *Phys. Rev. D* **73**, 092001 (2006).
- [30] J. P. Lees *et al.* (BABAR Collaboration), Measurement of angular asymmetries in the decays $B \rightarrow K^*\ell^+\ell^-$, *Phys. Rev. D* **93**, 052015 (2016).
- [31] J.-T. Wei *et al.* (Belle Collaboration), Measurement of the Differential Branching Fraction and Forward-Backward Asymmetry for $B \rightarrow K^{(*)}\ell^+\ell^-$, *Phys. Rev. Lett.* **103**, 171801 (2009).
- [32] S. Wehle *et al.* (Belle Collaboration), Lepton-Flavor-Dependent Angular Analysis of $B \rightarrow K^*\ell^+\ell^-$, *Phys. Rev. Lett.* **118**, 111801 (2017).
- [33] T. Aaltonen *et al.* (CDF Collaboration), Measurements of the Angular Distributions in the Decays $B \rightarrow K^{(*)}\mu^+\mu^-$ at CDF, *Phys. Rev. Lett.* **108**, 081807 (2012).
- [34] V. Khachatryan *et al.* (CMS Collaboration), Angular analysis of the decay $B^0 \rightarrow K^{*0}\mu^+\mu^-$ from pp collisions at $\sqrt{s} = 8 \text{ TeV}$, *Phys. Lett. B* **753**, 424 (2016).
- [35] A. M. Sirunyan *et al.* (CMS Collaboration), Measurement of angular parameters from the decay $B^0 \rightarrow K^{*0}\mu^+\mu^-$ in proton-proton collisions at $\sqrt{s} = 8 \text{ TeV}$, *Phys. Lett. B* **781**, 517 (2018).
- [36] R. Aaij *et al.* (LHCb Collaboration), Measurements of the S-wave fraction in $B^0 \rightarrow K^+\pi^-\mu^+\mu^-$ decays and the $B^0 \rightarrow K^*(892)^0\mu^+\mu^-$ differential branching fraction, *J. High Energy Phys.* **11** (2016) 047; **04** (2017) 142(E).
- [37] R. Aaij *et al.* (LHCb Collaboration), Branching Fraction Measurements of the rare $B_s^0 \rightarrow \phi\mu^+\mu^-$ and $B_s^0 \rightarrow f_2'(1525)\mu^+\mu^-$ Decays, *Phys. Rev. Lett.* **127**, 151801 (2021).
- [38] R. Aaij *et al.* (LHCb Collaboration), Differential branching fractions and isospin asymmetries of $B \rightarrow K^{(*)}\mu^+\mu^-$ decays, *J. High Energy Phys.* **06** (2014) 133.
- [39] R. Aaij *et al.* (LHCb Collaboration), Differential branching fraction and angular analysis of $\Lambda_b^0 \rightarrow \Lambda\mu^+\mu^-$ decays, *J. High Energy Phys.* **06** (2015) 115; **09** (2018) 145(E).
- [40] R. Aaij *et al.* (LHCb Collaboration), Measurement of lepton universality parameters in $B^+ \rightarrow K^+\ell^+\ell^-$ and $B^0 \rightarrow K^{*0}\ell^+\ell^-$ decays, arXiv:2212.09153 [Phys. Rev. D (to be published)].
- [41] M. Freytsis, Z. Ligeti, and J. T. Ruderman, Flavor models for $\bar{B} \rightarrow D^{(*)}\tau\bar{\nu}$, *Phys. Rev. D* **92**, 054018 (2015).
- [42] R. Benbrik and C.-H. Chen, Leptoquark on $P \rightarrow \ell^+\nu$, FCNC and LFV, *Phys. Lett. B* **672**, 172 (2009).
- [43] S. de Boer and G. Hiller, Flavor and new physics opportunities with rare charm decays into leptons, *Phys. Rev. D* **93**, 074001 (2016).
- [44] I. Doršner, S. Fajfer, A. Greljo, J. F. Kamenik, and N. Košnik, Physics of leptoquarks in precision experiments and at particle colliders, *Phys. Rep.* **641**, 1 (2016).
- [45] I. Doršner, S. Fajfer, and M. Patra, A comparative study of the S_1 and U_1 leptoquark effects in the light quark regime, *Eur. Phys. J. C* **80**, 204 (2020).
- [46] F. Abudinén, T. Blake, U. Egede, and T. Gershon, Prospects for studies of $D^{*0} \rightarrow \mu^+\mu^-$ and $B_{(s)}^{*0} \rightarrow \mu^+\mu^-$ decays, *Eur. Phys. J. C* **82**, 459 (2022).
- [47] Z. Kang and Y. Shigekami, $(g-2)_\mu$ versus flavor changing neutral current induced by the light $(B-L)_{\mu\tau}$ boson, *J. High Energy Phys.* **11** (2019) 049.
- [48] A. K. Alok, A. Dighe, S. Gangal, and D. Kumar, Predictions for $B_s \rightarrow \bar{K}^*\ell\ell$ in non-universal Z' models, *Eur. Phys. J. C* **80**, 682 (2020).
- [49] D. Guadagnoli, M. Reboud, and O. Sumensari, A gauged horizontal $SU(2)$ symmetry and $R_{K^{(*)}}$, *J. High Energy Phys.* **11** (2018) 163.
- [50] R. Alonso, A. Carmona, B. M. Dillon, J. F. Kamenik, J. M. Camalich, and J. Zupan, A clockwork solution to the flavor puzzle, *J. High Energy Phys.* **10** (2018) 099.
- [51] A. K. Alok, S. Banerjee, D. Kumar, S. U. Sankar, and D. London, New-physics signals of a model with a vector-singlet up-type quark, *Phys. Rev. D* **92**, 013002 (2015).
- [52] R. Aaij *et al.* (LHCb Collaboration), Search for the rare decay $D^0 \rightarrow \mu^+\mu^-$, *Phys. Lett. B* **725**, 15 (2013).
- [53] R. Aaij *et al.*, Performance of the LHCb trigger and full real-time reconstruction in Run 2 of the LHC, *J. Instrum.* **14**, P04013 (2019).
- [54] A. A. Alves Jr. *et al.* (LHCb Collaboration), The LHCb detector at the LHC, *J. Instrum.* **3**, S08005 (2008).
- [55] R. Aaij *et al.* (LHCb Collaboration), LHCb detector performance, *Int. J. Mod. Phys. A* **30**, 1530022 (2015).
- [56] T. Sjöstrand, S. Mrenna, and P. Skands, A brief introduction to PYTHIA 8.1, *Comput. Phys. Commun.* **178**, 852 (2008); PYTHIA 6.4 physics and manual, *J. High Energy Phys.* **05** (2006) 026.
- [57] I. Belyaev *et al.*, Handling of the generation of primary events in Gauss, the LHCb simulation framework, *J. Phys. Conf. Ser.* **331**, 032047 (2011).
- [58] D. J. Lange, The EvtGen particle decay simulation package, *Nucl. Instrum. Methods Phys. Res., Sect. A* **462**, 152 (2001).
- [59] S. Agostinelli *et al.* (Geant4 Collaboration), Geant4: A simulation toolkit, *Nucl. Instrum. Methods Phys. Res., Sect. A* **506**, 250 (2003).
- [60] J. Allison *et al.* (Geant4 Collaboration), Geant4 developments and applications, *IEEE Trans. Nucl. Sci.* **53**, 270 (2006).
- [61] M. Clemencic, G. Corti, S. Easo, C. R. Jones, S. Miglioranzi, M. Pappagallo, and P. Robbe, The LHCb simulation application, Gauss: Design, evolution and experience, *J. Phys. Conf. Ser.* **331**, 032023 (2011).
- [62] N. Davidson, T. Przedzinski, and Z. Was, PHOTOS interface in C++: Technical and physics documentation, *Comput. Phys. Commun.* **199**, 86 (2016).

- [63] W. D. Hulsbergen, Decay chain fitting with a Kalman filter, *Nucl. Instrum. Methods Phys. Res., Sect. A* **552**, 566 (2005).
- [64] L. Breiman, J. H. Friedman, R. A. Olshen, and C. J. Stone, *Classification and Regression Trees* (Wadsworth International Group, Belmont, California, USA, 1984).
- [65] Y. Freund and R. E. Schapire, A decision-theoretic generalization of on-line learning and an application to boosting, *J. Comput. Syst. Sci.* **55**, 119 (1997).
- [66] H. Voss, A. Hoecker, J. Stelzer, and F. Tegenfeldt, TMVA—Toolkit for multivariate data analysis with ROOT, *Proc. Sci.*, ACAT2007 (2007) 040.
- [67] A. Blum, A. Kalai, and J. Langford, Beating the hold-out: Bounds for k-fold and progressive cross-validation, in *Proceedings of the Twelfth Annual Conference on Computational Learning Theory, COLT '99*, (ACM, New York, NY, USA, 1999), p. 203.
- [68] R. Aaij *et al.*, Selection and processing of calibration samples to measure the particle identification performance of the LHCb experiment in Run 2, *Eur. Phys. J. Tech. Instr.* **6**, 1 (2019).
- [69] G. Punzi, Sensitivity of searches for new signals and its optimization, eConf **C030908**, MODT002 (2003), <https://inspirehep.net/literature/634798>.
- [70] Y. Amhis *et al.* (Heavy Flavor Averaging Group), Averages of b -hadron, c -hadron, and τ -lepton properties as of 2018, *Eur. Phys. J. C* **81**, 226 (2021), updated results and plots available at <https://hflav.web.cern.ch>.
- [71] R. Aaij *et al.* (LHCb Collaboration), Measurement of the track reconstruction efficiency at LHCb, *J. Instrum.* **10**, P02007 (2015).
- [72] S. Tolk, J. Albrecht, F. Dettori, and A. Pellegrino, Data driven trigger efficiency determination at LHCb, Reports No. LHCb-PUB-2014-039, No. CERN-LHCb-PUB-2014-039, CERN, Geneva, 2014.
- [73] R. Aaij *et al.* (LHCb Collaboration), Analysis of Neutral B -Meson Decays into Two Muons, *Phys. Rev. Lett.* **128**, 041801 (2022).
- [74] R. Aaij *et al.* (LHCb Collaboration), Measurement of the $B_s^0 \rightarrow \mu^+ \mu^-$ decay properties and search for the $B^0 \rightarrow \mu^+ \mu^-$ and $B_s^0 \rightarrow \mu^+ \mu^- \gamma$ decays, *Phys. Rev. D* **105**, 012010 (2022).
- [75] A. Martin Sanchez, P. Robbe, and M.-H. Schune, Performances of the LHCb L0 calorimeter trigger, Reports No. LHCb-PUB-2011-026, No. CERN-LHCb-PUB-2011-026, CERN, Geneva, 2012.
- [76] See Supplemental Material at <http://link.aps.org/supplemental/10.1103/PhysRevLett.131.041804> for additional figures.
- [77] T. Skwarnicki, A study of the radiative cascade transitions between the Upsilon-prime and UpsilonXn resonances, Ph.D. thesis, Institute of Nuclear Physics, Krakow, 1986 [Report No. DESY-F31-86-02].
- [78] N. L. Johnson, Systems of frequency curves generated by methods of translation, *Biometrika* **36**, 149 (1949).
- [79] A. L. Read, Presentation of search results: The CL_s technique, *J. Phys. G* **28**, 2693 (2002).
- [80] M. Kenzie *et al.*, GammaCombo: A statistical analysis framework for combining measurements, fitting datasets and producing confidence intervals, [10.5281/zenodo.3571421](https://zenodo.3571421).
- [81] R. Aaij *et al.* (LHCb Collaboration), Measurement of the CKM angle γ from a combination of LHCb results, *J. High Energy Phys.* **12** (2016) 087.

R. Aaij³², A. S. W. Abdelmotteleb⁵⁰, C. Abellan Beteta,⁴⁴ F. Abudinén⁵⁰, T. Ackernley⁵⁴, B. Adeva⁴⁰, M. Adinolfi⁴⁸, P. Adlarson⁷⁷, H. Afsharnia,⁹ C. Agapopoulou¹³, C. A. Aidala⁷⁸, S. Aiola²⁵, Z. Ajaltouni,⁹ S. Akar⁵⁹, K. Akiba³², J. Albrecht¹⁵, F. Alessio⁴², M. Alexander⁵³, A. Alfonso Albero³⁹, Z. Aliouche⁵⁶, P. Alvarez Cartelle⁴⁹, R. Amalric¹³, S. Amato², J. L. Amey⁴⁸, Y. Amhis^{11,42}, L. An⁴², L. Anderlini²², M. Andersson⁴⁴, A. Andreianov³⁸, M. Andreotti²¹, D. Andreou⁶², D. Ao⁶, F. Archilli¹⁷, A. Artamonov³⁸, M. Artuso⁶², E. Aslanides¹⁰, M. Atzeni⁴⁴, B. Audurier¹², S. Bachmann¹⁷, M. Bachmayer⁴³, J. J. Back⁵⁰, A. Bailly-reyre,¹³ P. Baladron Rodriguez⁴⁰, V. Balagura¹², W. Baldini²¹, J. Baptista de Souza Leite¹, M. Barbetti^{22,b}, R. J. Barlow⁵⁶, S. Barsuk¹¹, W. Barter⁵⁵, M. Bartolini⁴⁹, F. Baryshnikov³⁸, J. M. Basels¹⁴, G. Bassi^{29,c}, B. Batskh⁴, A. Battig¹⁵, A. Bay⁴³, A. Beck⁵⁰, M. Becker¹⁵, F. Bedeschi²⁹, I. B. Bediaga¹, A. Beiter,⁶² V. Belavin,³⁸ S. Belin⁴⁰, V. Bellee⁴⁴, K. Belous³⁸, I. Belov³⁸, I. Belyaev³⁸, G. Benane¹⁰, G. Bencivenni²³, E. Ben-Haim¹³, A. Berezhnoy³⁸, R. Bernet⁴⁴, S. Bernet Andres⁷⁶, D. Berninghoff,¹⁷ H. C. Bernstein,⁶² C. Bertella⁵⁶, A. Bertolin²⁸, C. Betancourt⁴⁴, F. Bettin⁴², Ia. Bezshyiko⁴⁴, S. Bhasin⁴⁸, J. Bhom³⁵, L. Bian⁶⁸, M. S. Bieker¹⁵, N. V. Biesuz²¹, S. Bifani⁴⁷, P. Billoir¹³, A. Biolchini³², M. Birch⁵⁵, F. C. R. Bishop⁴⁹, A. Bitadze⁵⁶, A. Bizzeti⁴⁰, M. P. Blago⁴⁹, T. Blake⁵⁰, F. Blanc⁴³, J. E. Blank¹⁵, S. Blusk⁶², D. Bobulska⁵³, J. A. Boelhauve¹⁵, O. Boente Garcia¹², T. Boettcher⁵⁹, A. Boldyrev³⁸, C. S. Bolognani⁷⁴, R. Bolzonella^{21,d}, N. Bondar^{38,42}, F. Borgato²⁸, S. Borghi⁵⁶, M. Borsato¹⁷, J. T. Borsuk³⁵, S. A. Bouchiba⁴³, T. J. V. Bowcock⁵⁴, A. Boyer⁴², C. Bozzi²¹, M. J. Bradley,⁵⁵ S. Braun⁶⁰, A. Brea Rodriguez⁴⁰, J. Brodzicka³⁵, A. Brossa Gonzalo⁴⁰, J. Brown⁵⁴, D. Brundu²⁷, A. Buonauro⁴⁴, L. Buonincontri²⁸, A. T. Burke⁵⁶, C. Burr⁴², A. Bursche,⁶⁶ A. Butkevich³⁸, J. S. Butter³², J. Buytaert⁴², W. Byczynski⁴², S. Cadeddu²⁷, H. Cai,⁶⁸

- R. Calabrese^{21,d} L. Calefice¹⁵ S. Cali²³ R. Calladine⁴⁷ M. Calvi^{26,e} M. Calvo Gomez⁷⁶ P. Campana²³
D. H. Campora Perez⁷⁴ A. F. Campoverde Quezada⁶ S. Capelli^{26,e} L. Capriotti²⁰ A. Carbone^{20,f} G. Carboni³¹
R. Cardinale^{24,g} A. Cardini²⁷ P. Carniti^{26,e} L. Carus,¹⁴ A. Casais Vidal⁴⁰ R. Caspary¹⁷ G. Casse⁵⁴
M. Cattaneo⁴² G. Cavallero⁴² V. Cavallini^{21,d} S. Celani⁴³ J. Cerasoli¹⁰ D. Cervenkov⁵⁷ A. J. Chadwick⁵⁴
M. G. Chapman⁴⁸ M. Charles¹³ Ph. Charpentier⁴² C. A. Chavez Barajas⁵⁴ M. Chefdeville⁸ C. Chen³
S. Chen⁴ A. Chernov³⁵ S. Chernyshenko⁴⁶ V. Chobanova⁴⁰ S. Cholak⁴³ M. Chrzaszcz³⁵ A. Chubykin³⁸
V. Chulikov³⁸ P. Ciambrone²³ M. F. Cicala⁵⁰ X. Cid Vidal⁴⁰ G. Ciezarek⁴² G. Ciullo^{21,d} P. E. L. Clarke⁵²
M. Clemencic⁴² H. V. Cliff⁴⁹ J. Closier⁴² J. L. Cobbledick⁵⁶ V. Coco⁴² J. A. B. Coelho¹¹ J. Cogan¹⁰
E. Cogneras⁹ L. Cojocariu³⁷ P. Collins⁴² T. Colombo⁴² L. Congedo¹⁹ A. Contu²⁷ N. Cooke⁴⁷
I. Corredoira⁴⁰ G. Corti⁴² B. Couturier⁴² D. C. Craik⁴⁴ M. Cruz Torres^{1,h} R. Currie⁵² C. L. Da Silva⁶¹
S. Dadabaev³⁸ L. Dai⁶⁵ X. Dai⁵ E. Dall'Occo¹⁵ J. Dalseno⁴⁰ C. D'Ambrosio⁴² J. Daniel⁹ A. Danilina³⁸
P. d'Argent¹⁵ J. E. Davies⁵⁶ A. Davis⁵⁶ O. De Aguiar Francisco⁵⁶ J. de Boer⁴² K. De Bruyn⁷³ S. De Capua⁵⁶
M. De Cian⁴³ U. De Freitas Carneiro Da Graca¹ E. De Lucia²³ J. M. De Miranda¹ L. De Paula² M. De Serio^{19,i}
D. De Simone⁴⁴ P. De Simone²³ F. De Vellis¹⁵ J. A. de Vries⁷⁴ C. T. Dean⁶¹ F. Debernardis^{19,j} D. Decamp⁸
V. Dedu¹⁰ L. Del Buono¹³ B. Delaney⁵⁸ H.-P. Dembinski¹⁵ V. Denysenko⁴⁴ O. Deschamps⁹ F. Dettori⁸
B. Dey⁷¹ P. Di Nezza²³ I. Diachkov³⁸ S. Didenko³⁸ L. Dieste Maronas⁴⁰ S. Ding⁶² V. Dobishuk⁴⁶
A. Dolmatov³⁸ C. Dong³ A. M. Donohoe¹⁸ F. Dordei²⁷ A. C. dos Reis¹ L. Douglas⁵³ A. G. Downes⁸
P. Duda⁷⁵ M. W. Dudek³⁵ L. Dufour⁴² V. Duk⁷² P. Durante⁴² M. M. Duras⁷⁵ J. M. Durham⁶¹ D. Dutta⁵⁶
A. Dziurda³⁵ A. Dzyuba³⁸ S. Easo⁵¹ U. Egede⁶³ V. Egorychev³⁸ S. Eidelman^{38,a} C. Eirea Orro⁴⁰
S. Eisenhardt⁵² E. Ejopu⁵⁶ S. Ek-In⁴³ L. Eklund⁷⁷ S. Ely⁶² A. Ene³⁷ E. Epple⁵⁹ S. Escher¹⁴ J. Eschle⁴⁴
S. Esen⁴⁴ T. Evans⁵⁶ F. Fabiano^{27,j} L. N. Falcao¹ Y. Fan⁶ B. Fang^{11,68} L. Fantini^{72,k} M. Faria⁴³
S. Farry⁵⁴ D. Fazzini^{26,e} L. F. Felkowski⁷⁵ M. Feo⁴² M. Fernandez Gomez⁴⁰ A. D. Fernez⁶⁰ F. Ferrari²⁰
L. Ferreira Lopes⁴³ F. Ferreira Rodrigues² S. Ferreres Sole³² M. Ferrillo⁴⁴ M. Ferro-Luzzi⁴² S. Filippov³⁸
R. A. Fini¹⁹ M. Fiorini^{21,d} M. Firlej⁵⁷ K. M. Fischer⁷⁸ D. S. Fitzgerald⁵⁶ C. Fitzpatrick⁵⁶ T. Fiutowski³⁴
F. Fleuret¹² M. Fontana¹³ F. Fontanelli^{24,g} R. Forty⁴² D. Foulds-Holt⁴⁹ V. Franco Lima⁵⁴
M. Franco Sevilla⁶⁰ M. Frank⁴² E. Franzoso^{21,d} G. Frau¹⁷ C. Frei⁴² D. A. Friday⁵³ J. Fu⁶ Q. Fuehring¹⁵
T. Fulghesu¹³ E. Gabriel³² G. Galati^{19,i} M. D. Galati³² A. Gallas Torreira⁴⁰ D. Galli^{20,f} S. Gambetta^{52,42}
Y. Gan³ M. Gandelman² P. Gandini²⁵ Y. Gao⁷ Y. Gao⁵ M. Garau^{27,j} L. M. Garcia Martin⁵⁰
P. Garcia Moreno³⁹ J. Garcia Pardiñas^{26,e} B. Garcia Plana⁴⁰ F. A. Garcia Rosales¹² L. Garrido³⁹ C. Gaspar⁴²
R. E. Geertsema³² D. Gerick¹⁷ L. L. Gerken¹⁵ E. Gersabeck⁵⁶ M. Gersabeck⁵⁶ T. Gershon⁵⁰
L. Giambastiani²⁸ V. Gibson⁴⁹ H. K. Giemza³⁶ A. L. Gilman⁵⁷ M. Giovannetti^{23,l} A. Gioventù⁴⁰
P. Gironella Gironell³⁹ C. Giugliano^{21,d} M. A. Giza³⁵ K. Gizzov⁵² E. L. Gkougkousis⁴² V. V. Gligorov^{13,42}
C. Göbel⁶⁴ E. Golobardes⁷⁶ D. Golubkov³⁸ A. Golutvin^{55,38} A. Gomes^{1,m} S. Gomez Fernandez³⁹
F. Goncalves Abrantes⁵⁷ M. Goncerz³⁵ G. Gong³ I. V. Gorelov³⁸ C. Gotti²⁶ J. P. Grabowski⁷⁰
T. Grammatico¹³ L. A. Granado Cardoso⁴² E. Graugés³⁹ E. Graverini⁴³ G. Graziani⁴² A. T. Grecu³⁷
L. M. Greeven³² N. A. Grieser⁴ L. Grillo⁵³ S. Gromov³⁸ B. R. Gruberg Cazon⁵⁷ C. Gu³ M. Guarise^{21,d}
M. Guittiere¹¹ P. A. Günther¹⁷ E. Gushchin³⁸ A. Guth¹⁴ Y. Guz³⁸ T. Gys⁴² T. Hadavizadeh⁶³
C. Hadjivasilou⁶⁰ G. Haefeli⁴³ C. Haen⁴² J. Haimberger⁴² S. C. Haines⁴⁹ T. Halewood-leagas⁵⁴
M. M. Halvorsen⁴² P. M. Hamilton⁶⁰ J. Hammerich⁴² Q. Han⁷ X. Han¹⁷ E. B. Hansen⁵⁶
S. Hansmann-Menzemer¹⁷ L. Hao⁶ N. Harnew⁵⁷ T. Harrison⁵⁴ C. Hasse⁴² M. Hatch⁴² J. He^{6,n}
K. Heijhoff³² C. Henderson⁵⁹ R. D. L. Henderson^{63,50} A. M. Hennequin⁵⁸ K. Hennessy⁴² L. Henry⁴²
J. Herd⁵⁵ J. Heuel¹⁴ A. Hicheur² D. Hill⁴³ M. Hilton⁵⁶ S. E. Hollitt¹⁵ J. Horswill⁵⁶ R. Hou⁷ Y. Hou⁸
J. Hu¹⁷ J. Hu⁶⁶ W. Hu⁵ X. Hu³ W. Huang⁶ X. Huang⁶⁸ W. Hulsbergen³² R. J. Hunter⁵⁰ M. Hushchyn³⁸
D. Hutchcroft⁵⁴ P. Ibis¹⁵ M. Idzik³⁴ D. Ilin³⁸ P. Ilten⁵⁹ A. Inglessi³⁸ A. Iniuksin³⁸ A. Ishteev³⁸
K. Ivshin³⁸ R. Jacobsson⁴² H. Jage¹⁴ S. J. Jaimes Elles⁴¹ S. Jakobsen⁴² E. Jans³² B. K. Jashal⁴¹
A. Jawahery⁶⁰ V. Jevtic¹⁵ E. Jiang⁶⁰ X. Jiang^{4,6} Y. Jiang⁶ M. John⁵⁷ D. Johnson⁵⁸ C. R. Jones⁴⁹
T. P. Jones⁵⁰ B. Jost⁴² N. Jurik⁴² I. Juszczak³⁵ S. Kandybei⁴⁵ Y. Kang³ M. Karacson⁴² D. Karpenkov³⁸
M. Karpov³⁸ J. W. Kautz⁵⁹ F. Keizer⁴² D. M. Keller⁶² M. Kenzie⁵⁰ T. Ketel³² B. Khanji¹⁵ A. Kharisova³⁸
S. Kholodenko^{38,38} G. Khreich¹¹ T. Kirn¹⁴ V. S. Kirsebom⁴³ O. Kitouni⁵⁸ S. Klaver³³ N. Kleijne^{29,c}

- K. Klimaszewski³⁶ M. R. Kmiec³⁶ S. Koliiev⁴⁶ A. Kondybayeva³⁸ A. Konoplyannikov³⁸ P. Kopciewicz³⁴
 R. Kopecna,¹⁷ P. Koppenburg³² M. Korolev³⁸ I. Kostiuk^{32,46} O. Kot,⁴⁶ S. Kotriakhova³⁸ A. Kozachuk³⁸
 P. Kravchenko³⁸ L. Kravchuk³⁸ R. D. Krawczyk⁴² M. Kreps⁵⁰ S. Kretzschmar¹⁴ P. Krokovny³⁸
 W. Krupa³⁴ W. Krzemien³⁶ J. Kubat,¹⁷ S. Kubis⁷⁵ W. Kucewicz^{35,34} M. Kucharczyk³⁵ V. Kudryavtsev³⁸
 A. Kupsc⁷⁷ D. Lacarrere⁴² G. Lafferty⁵⁶ A. Lai²⁷ A. Lampis^{27,j} D. Lancierini⁴⁴ C. Landesa Gomez⁴⁰
 J. J. Lane⁵⁶ R. Lane⁴⁸ G. Lanfranchi²³ C. Langenbruch¹⁴ J. Langer¹⁵ O. Lantwin³⁸ T. Latham⁵⁰
 F. Lazzari^{29,o} M. Lazzaroni^{25,p} R. Le Gac¹⁰ S. H. Lee⁷⁸ R. Lefevre⁹ A. Leflat³⁸ S. Legotin³⁸ P. Lenisa^{21,d}
 O. Leroy¹⁰ T. Lesiak³⁵ B. Leverington¹⁷ A. Li³ H. Li⁶⁶ K. Li⁷ P. Li¹⁷ P.-R. Li⁶⁷ S. Li⁷ T. Li⁴ T. Li⁶⁶
 Y. Li⁴ Z. Li⁶² X. Liang⁶² C. Lin⁶ T. Lin⁵¹ R. Lindner⁴² V. Lisovskyi¹⁵ R. Litvinov^{27,j} G. Liu⁶⁶
 H. Liu⁶ Q. Liu⁶ S. Liu^{4,6} A. Lobo Salvia³⁹ A. Loi²⁷ R. Lollini⁷² J. Lomba Castro⁴⁰ I. Longstaff,⁵³
 J. H. Lopes² A. Lopez Huertas³⁹ S. López Soliño⁴⁰ G. H. Lovell⁴⁹ Y. Lu^{4,q} C. Lucarelli^{22,b} D. Lucchesi^{28,r}
 S. Luchuk³⁸ M. Lucio Martinez⁷⁴ V. Lukashenko^{32,46} Y. Luo³ A. Lupato⁵⁶ E. Luppi^{21,d} A. Lusiani^{29,c}
 K. Lynch¹⁸ X.-R. Lyu⁶ L. Ma⁴ R. Ma⁶ S. Maccolini²⁰ F. Machefert¹¹ F. Maciuc³⁷ I. Mackay⁵⁷
 V. Macko⁴³ P. Mackowiak¹⁵ L. R. Madhan Mohan⁴⁸ A. Maevskiy³⁸ D. Maisuzenko³⁸ M. W. Majewski,³⁴
 J. J. Malczewski³⁵ S. Malde⁵⁷ B. Malecki^{35,42} A. Malinin³⁸ T. Maltsev^{38,38} G. Manca^{27,j} G. Mancinelli¹⁰
 C. Mancuso^{11,25,p} D. Manuzzi²⁰ C. A. Manzari⁴⁴ D. Marangotto^{25,p} J. F. Marchand⁸ U. Marconi²⁰
 S. Mariani^{22,b} C. Marin Benito³⁹ J. Marks¹⁷ A. M. Marshall⁴⁸ P. J. Marshall⁵⁴ G. Martelli^{72,k} G. Martellotti³⁰
 L. Martinazzoli^{42,e} M. Martinelli^{26,e} D. Martinez Santos⁴⁰ F. Martinez Vidal⁴¹ A. Massafferri¹ M. Materok¹⁴
 R. Matev⁴² A. Mathad⁴⁴ V. Matiunin³⁸ C. Matteuzzi²⁶ K. R. Mattioli¹² A. Mauri³² E. Maurice¹²
 J. Mauricio³⁹ M. Mazurek⁴² M. McCann⁵⁵ L. McConnell¹⁸ T. H. McGrath⁵⁶ N. T. McHugh⁵³ A. McNab⁵⁶
 R. McNulty¹⁸ J. V. Mead⁵⁴ B. Meadows⁵⁹ G. Meier¹⁵ D. Melnychuk³⁶ S. Meloni^{26,e} M. Merk^{32,74}
 A. Merli^{25,p} L. Meyer Garcia² D. Miao^{4,6} M. Mikhasenko^{70,s} D. A. Milanes⁶⁹ E. Millard,⁵⁰ M. Milovanovic⁴²
 M.-N. Minard,^{8,a} A. Minotti^{26,e} T. Miralles⁹ S. E. Mitchell⁵² B. Mitreska⁵⁶ D. S. Mitzel¹⁵ A. Mödden¹⁵
 R. A. Mohammed⁵⁷ R. D. Moise¹⁴ S. Mokhnenko³⁸ T. Mombächer⁴⁰ M. Monk^{50,63} I. A. Monroy⁶⁹
 S. Monteil⁹ M. Morandin²⁸ G. Morello²³ M. J. Morello^{29,c} J. Moron³⁴ A. B. Morris⁷⁰ A. G. Morris⁵⁰
 R. Mountain⁶² H. Mu³ E. Muhammad⁵⁰ F. Muheim⁵² M. Mulder⁷³ K. Müller⁴⁴ C. H. Murphy⁵⁷
 D. Murray⁵⁶ R. Murta⁵⁵ P. Muzzetto^{27,j} P. Naik⁴⁸ T. Nakada⁴³ R. Nandakumar⁵¹ T. Nanut⁴² I. Nasteva²
 M. Needham⁵² N. Neri^{25,p} S. Neubert⁷⁰ N. Neufeld⁴² P. Neustroeve³⁸ R. Newcombe,⁵⁵ J. Nicolini^{15,11}
 E. M. Niel⁴³ S. Nieswand,¹⁴ N. Nikitin³⁸ N. S. Nolte⁵⁸ C. Normand^{8,27,j} J. Novoa Fernandez⁴⁰ C. Nunez⁷⁸
 A. Oblakowska-Mucha³⁴ V. Obraztsov³⁸ T. Oeser¹⁴ D. P. O'Hanlon⁴⁸ S. Okamura^{21,d} R. Oldeman^{27,j}
 F. Oliva⁵² C. J. G. Onderwater⁷³ R. H. O'Neil⁵² J. M. Otalora Goicochea² T. Ovsianikova³⁸ P. Owen⁴⁴
 A. Oyanguren⁴¹ O. Ozcelik⁵² K. O. Padeken⁷⁰ B. Pagare⁵⁰ P. R. Pais⁴² T. Pajero⁵⁷ A. Palano¹⁹
 M. Palutan²³ Y. Pan⁵⁶ G. Panshin³⁸ L. Paolucci⁵⁰ A. Papanestis⁵¹ M. Pappagallo^{19,i} L. L. Pappalardo^{21,d}
 C. Pappenheimer⁵⁹ W. Parker⁶⁰ C. Parkes⁵⁶ B. Passalacqua^{21,d} G. Passaleva²² A. Pastore¹⁹ M. Patel¹⁹
 C. Patrignani^{20,f} C. J. Pawley⁷⁴ A. Pearce⁴² A. Pellegrino³² M. Pepe Altarelli⁴² S. Perazzini²⁰ D. Pereima³⁸
 A. Pereiro Castro⁴⁰ P. Perret⁹ M. Petric,⁵³ K. Petridis⁴⁸ A. Petrolini^{24,g} A. Petrov,³⁸ S. Petrucci⁵² M. Petruzzo²⁵
 H. Pham⁶² A. Philippov³⁸ R. Piandani⁶ L. Pica^{29,c} M. Piccini⁷² B. Pietrzyk⁸ G. Pietrzyk¹¹ M. Pili⁵⁷
 D. Pinci³⁰ F. Pisani⁴² M. Pizzichemi^{26,42,e} V. Placinta³⁷ J. Plews⁴⁷ M. Plo Casasus⁴⁰ F. Polci^{13,42}
 M. Poli Lener²³ M. Poliakova,⁶² A. Poluektov¹⁰ N. Polukhina^{38,38} I. Polyakov⁴² E. Polycarpo² S. Ponce⁴²
 D. Popov^{6,42} S. Popov³⁸ S. Poslavskii³⁸ K. Prasanth³⁵ L. Promberger¹⁷ C. Prouve⁴⁰ V. Pugatch⁴⁶
 V. Puill¹¹ G. Punzi^{29,t} H. R. Qi³ W. Qian⁶ N. Qin³ S. Qu³ R. Quagliani⁴³ N. V. Raab¹⁸
 R. I. Rabadan Trejo,⁶ B. Rachwal³⁴ J. H. Rademacker⁴⁸ R. Rajagopalan,⁶² M. Rama²⁹ M. Ramos Pernas⁵⁰
 M. S. Rangel² F. Ratnikov^{38,38} G. Raven^{33,42} M. Rebollo De Miguel⁴¹ F. Redi⁴² J. Reich⁴⁸ F. Reiss¹⁹
 C. Remon Alepuz,⁴¹ Z. Ren³ P. K. Resmi¹⁰ R. Ribatti^{29,c} A. M. Ricci²⁷ S. Ricciardi⁵¹ K. Richardson⁵⁸
 M. Richardson-Slipper⁵² K. Rinnert⁵⁴ P. Robbe¹¹ G. Robertson⁵² A. B. Rodrigues⁴³ E. Rodrigues⁵⁴
 E. Rodriguez Fernandez⁴⁰ J. A. Rodriguez Lopez⁶⁹ E. Rodriguez Rodriguez⁴⁰ D. L. Rolf⁴² A. Rollings⁵⁷
 P. Roloff⁴² V. Romanovskiy³⁸ M. Romero Lamas⁴⁰ A. Romero Vidal⁴⁰ J. D. Roth,^{78,a} M. Rotondo²³
 M. S. Rudolph⁶² T. Ruf⁴² R. A. Ruiz Fernandez⁴⁰ J. Ruiz Vidal,⁴¹ A. Ryzhikov³⁸ J. Ryzka³⁴
 J. J. Saborido Silva⁴⁰ N. Sagidova³⁸ N. Sahoo⁴⁷ B. Saitta^{27,j} M. Salomoni⁴² C. Sanchez Gras³²

- I. Sanderswood¹,⁴¹ R. Santacesaria²,³⁰ C. Santamarina Rios³,⁴⁰ M. Santimaria⁴,²³ E. Santovetti⁵,^{31,l} D. Saranin⁶,³⁸ G. Sarpis⁷,¹⁴ M. Sarpis⁸,⁷⁰ A. Sarti⁹,^{30,u} C. Satriano¹⁰,^{30,u} A. Satta¹¹,³¹ M. Saur¹²,¹⁵ D. Savrina¹³,^{38,38} H. Sazak¹⁴,⁹ L. G. Scantlebury Smead¹⁵,⁵⁷ A. Scarabotto¹⁶,¹³ S. Schael¹⁷,¹⁴ S. Scherl¹⁸,⁵⁴ M. Schiller¹⁹,⁵³ H. Schindler²⁰,⁴² M. Schmelling²¹,¹⁶ B. Schmidt²²,⁴² S. Schmitt²³,¹⁴ O. Schneider²⁴,⁴³ A. Schopper²⁵,⁴² M. Schubiger²⁶,³² S. Schulte²⁷,⁴³ M. H. Schune²⁸,¹¹ R. Schwemmer²⁹,⁴² B. Sciascia³⁰,^{23,42} A. Sciuccati³¹,⁴² S. Sellam³²,⁴⁰ A. Semennikov³³,³⁸ M. Senghi Soares³⁴,³³ A. Sergi³⁵,^{24,g} N. Serra³⁶,⁴⁴ L. Sestini³⁷,²⁸ A. Seuthe³⁸,¹⁵ Y. Shang³⁹,⁵ D. M. Shangase⁴⁰,⁷⁸ M. Shapkin⁴¹,³⁸ I. Shchemberov⁴²,³⁸ L. Shchutska⁴³,⁴³ T. Shears⁴⁴,⁵⁴ L. Shekhtman⁴⁵,³⁸ Z. Shen⁴⁶,⁵ S. Sheng⁴⁷,^{4,6} V. Shevchenko⁴⁸,³⁸ B. Shi⁴⁹,⁶ E. B. Shields⁵⁰,^{26,e} Y. Shimizu⁵¹,¹¹ E. Shmanin⁵²,³⁸ R. Shorkin⁵³,³⁸ J. D. Shupperd⁵⁴,⁶² B. G. Siddi⁵⁵,^{21,d} R. Silva Coutinho⁵⁶,⁶² G. Simi⁵⁷,²⁸ S. Simone⁵⁸,^{19,i} M. Singla⁵⁹,⁶³ N. Skidmore⁶⁰,⁵⁶ R. Skuza⁶¹,¹⁷ T. Skwarnicki⁶²,⁶² M. W. Slater⁶³,⁴⁷ J. C. Smallwood⁶⁴,⁵⁷ J. G. Smeaton⁶⁵,⁴⁹ E. Smith⁶⁶,⁴⁴ K. Smith⁶⁷,⁶¹ M. Smith⁶⁸,⁵⁵ A. Snoch⁶⁹,³² L. Soares Lavra⁷⁰,⁹ M. D. Sokoloff⁷¹,⁵⁹ F. J. P. Soler⁷²,⁵³ A. Solomin⁷³,^{38,48} A. Solovev⁷⁴,³⁸ I. Solovyev⁷⁵,³⁸ R. Song⁷⁶,⁶³ F. L. Souza De Almeida⁷⁷,² B. Souza De Paula⁷⁸,² B. Spaan⁷⁹,^{15,a} E. Spadaro Norella⁸⁰,^{25,p} E. Spedicato⁸¹,²⁰ E. Spiridenkov⁸²,³⁸ P. Spradlin⁸³,⁵³ V. Sriskaran⁸⁴,⁴² F. Stagni⁸⁵,⁴² M. Stahl⁸⁶,⁴² S. Stahl⁸⁷,⁴² S. Stanislaus⁸⁸,⁵⁷ E. N. Stein⁸⁹,⁴² O. Steinkamp⁹⁰,⁴⁴ O. Stenyakin⁹¹,³⁸ H. Stevens⁹²,¹⁵ S. Stone⁹³,^{62,a} D. Strekalina⁹⁴,³⁸ Y. S Su⁹⁵,⁶ F. Suljik⁹⁶,⁵⁷ J. Sun⁹⁷,²⁷ L. Sun⁹⁸,⁶⁸ Y. Sun⁹⁹,⁶⁰ P. Svihra¹⁰⁰,⁵⁶ P. N. Swallow¹⁰¹,⁴⁷ K. Swientek¹⁰²,³⁴ A. Szabelski¹⁰³,³⁶ T. Szumlak¹⁰⁴,³⁴ M. Szymanski¹⁰⁵,⁴² Y. Tan¹⁰⁶,³ S. Taneja¹⁰⁷,⁵⁶ A. R. Tanner¹⁰⁸,⁴⁸ M. D. Tat¹⁰⁹,⁵⁷ A. Terentev¹¹⁰,³⁸ F. Teubert¹¹¹,⁴² E. Thomas¹¹²,⁴² D. J. D. Thompson¹¹³,⁴⁷ K. A. Thomson¹¹⁴,⁵⁴ H. Tilquin¹¹⁵,⁵⁵ V. Tisserand¹¹⁶,⁹ S. T'Jampens¹¹⁷,⁸ M. Tobin¹¹⁸,⁴ L. Tomassetti¹¹⁹,^{21,d} G. Tonani¹²⁰,^{25,p} X. Tong¹²¹,⁵ D. Torres Machado¹²²,¹ D. Y. Tou¹²³,³ S. M. Trilov¹²⁴,⁴⁸ C. Trippel¹²⁵,⁴³ G. Tuci¹²⁶,⁶ A. Tully¹²⁷,⁴³ N. Tuning¹²⁸,³² A. Ukleja¹²⁹,³⁶ D. J. Unverzagt¹³⁰,¹⁷ A. Usachov¹³¹,³² A. Ustyuzhanin¹³²,^{38,38} U. Uwer¹³³,¹⁷ A. Vagner¹³⁴,³⁸ V. Vagnoni¹³⁵,²⁰ A. Valassi¹³⁶,⁴² G. Valenti¹³⁷,²⁰ N. Valls Canudas¹³⁸,⁷⁶ M. van Beuzekom¹³⁹,³² M. Van Dijk¹⁴⁰,⁴³ H. Van Hecke¹⁴¹,⁶¹ E. van Herwijnen¹⁴²,⁵⁵ C. B. Van Hulse¹⁴³,^{40,v} M. van Veghel¹⁴⁴,⁷³ R. Vazquez Gomez¹⁴⁵,³⁹ P. Vazquez Regueiro¹⁴⁶,⁴⁰ C. Vázquez Sierra¹⁴⁷,⁴² S. Vecchi¹⁴⁸,²¹ J. J. Velthuis¹⁴⁹,⁴⁸ M. Veltri¹⁵⁰,^{22,w} A. Venkateswaran¹⁵¹,⁴³ M. Veronesi¹⁵²,³² M. Vesterinen¹⁵³,⁵⁰ D. Vieira¹⁵⁴,⁵⁹ M. Vieites Diaz¹⁵⁵,⁴³ X. Vilasis-Cardona¹⁵⁶,⁷⁶ E. Vilella Figueras¹⁵⁷,⁵⁴ A. Villa¹⁵⁸,²⁰ P. Vincent¹⁵⁹,¹³ F. C. Volle¹⁶⁰,¹¹ D. vom Bruch¹⁶¹,¹⁰ A. Vorobyev¹⁶²,³⁸ V. Vorobyev¹⁶³,³⁸ N. Voropaev¹⁶⁴,³⁸ K. Vos¹⁶⁵,⁷⁴ C. Vradas¹⁶⁶,⁵² R. Waldi¹⁶⁷,¹⁷ J. Walsh¹⁶⁸,²⁹ G. Wan¹⁶⁹,⁵ C. Wang¹⁷⁰,¹⁷ G. Wang¹⁷¹,⁷ J. Wang¹⁷²,⁵ J. Wang¹⁷³,⁴ J. Wang¹⁷⁴,³ J. Wang¹⁷⁵,⁶⁸ M. Wang¹⁷⁶,⁵ R. Wang¹⁷⁷,⁴⁸ X. Wang¹⁷⁸,⁶⁶ Y. Wang¹⁷⁹,⁷ Z. Wang¹⁸⁰,⁴⁴ Z. Wang¹⁸¹,³ Z. Wang¹⁸²,⁶ J. A. Ward¹⁸³,^{50,63} N. K. Watson¹⁸⁴,⁴⁷ D. Websdale¹⁸⁵,⁵⁵ Y. Wei¹⁸⁶,⁵ C. Weisser¹⁸⁷,⁵⁸ B. D. C. Westhenry¹⁸⁸,⁴⁸ D. J. White¹⁸⁹,⁵⁶ M. Whitehead¹⁹⁰,⁵³ A. R. Wiederhold¹⁹¹,⁵⁰ D. Wiedner¹⁹²,¹⁵ G. Wilkinson¹⁹³,⁵⁷ M. K. Wilkinson¹⁹⁴,⁵⁹ I. Williams¹⁹⁵,⁴⁹ M. Williams¹⁹⁶,⁵⁸ M. R. J. Williams¹⁹⁷,⁵² R. Williams¹⁹⁸,⁴⁹ F. F. Wilson¹⁹⁹,⁵¹ W. Wislicki²⁰⁰,³⁶ M. Witek²⁰¹,³⁵ L. Witola²⁰²,¹⁷ C. P. Wong²⁰³,⁶¹ G. Wormser²⁰⁴,¹¹ S. A. Wotton²⁰⁵,⁴⁹ H. Wu²⁰⁶,⁶² J. Wu²⁰⁷,⁷ K. Wyllie²⁰⁸,⁴² Z. Xiang²⁰⁹,⁶ D. Xiao²¹⁰,⁷ Y. Xie²¹¹,⁷ A. Xu²¹²,⁵ J. Xu²¹³,⁶ L. Xu²¹⁴,³ L. Xu²¹⁵,³ M. Xu²¹⁶,⁵⁰ Q. Xu²¹⁷,⁶ Z. Xu²¹⁸,⁹ Z. Xu²¹⁹,⁶ D. Yang²²⁰,³ S. Yang²²¹,⁶ X. Yang²²²,⁵ Y. Yang²²³,⁶ Z. Yang²²⁴,⁵ Z. Yang²²⁵,⁶⁰ L. E. Yeomans²²⁶,⁵⁴ V. Yeroshenko²²⁷,¹¹ H. Yeung²²⁸,⁵⁶ H. Yin²²⁹,⁷ J. Yu²³⁰,⁶⁵ X. Yuan²³¹,⁶² E. Zaffaroni²³²,⁴³ M. Zavertyaev²³³,¹⁶ M. Zdybal²³⁴,³⁵ O. Zenaiev²³⁵,⁴² M. Zeng²³⁶,³ C. Zhang²³⁷,⁵ D. Zhang²³⁸,⁷ L. Zhang²³⁹,³ S. Zhang²⁴⁰,⁶⁵ S. Zhang²⁴¹,⁵ Y. Zhang²⁴²,⁵ Y. Zhang²⁴³,⁵⁷ A. Zharkova²⁴⁴,³⁸ A. Zhelezov²⁴⁵,¹⁷ Y. Zheng²⁴⁶,⁶ T. Zhou²⁴⁷,⁵ X. Zhou²⁴⁸,⁶ Y. Zhou²⁴⁹,⁶ V. Zhokovska²⁵⁰,¹¹ X. Zhu²⁵¹,³ X. Zhu²⁵²,⁷ Z. Zhu²⁵³,⁶ V. Zhukov²⁵⁴,^{14,38} Q. Zou²⁵⁵,^{4,6} S. Zucchelli²⁵⁶,^{20,f} D. Zuliani²⁵⁷,²⁸ and G. Zunica²⁵⁸

(LHCb Collaboration)

¹Centro Brasileiro de Pesquisas Físicas (CBPF), Rio de Janeiro, Brazil²Universidade Federal do Rio de Janeiro (UFRJ), Rio de Janeiro, Brazil³Center for High Energy Physics, Tsinghua University, Beijing, China⁴Institute Of High Energy Physics (IHEP), Beijing, China⁵School of Physics State Key Laboratory of Nuclear Physics and Technology, Peking University, Beijing, China⁶University of Chinese Academy of Sciences, Beijing, China⁷Institute of Particle Physics, Central China Normal University, Wuhan, Hubei, China⁸Université Savoie Mont Blanc, CNRS, IN2P3-LAPP, Annecy, France⁹Université Clermont Auvergne, CNRS/IN2P3, LPC, Clermont-Ferrand, France¹⁰Aix Marseille Univ, CNRS/IN2P3, CPPM, Marseille, France¹¹Université Paris-Saclay, CNRS/IN2P3, IJCLab, Orsay, France

- ¹²Laboratoire Leprince-Ringuet, CNRS/IN2P3, Ecole Polytechnique, Institut Polytechnique de Paris, Palaiseau, France
¹³LPNHE, Sorbonne Université, Paris Diderot Sorbonne Paris Cité, CNRS/IN2P3, Paris, France
¹⁴I. Physikalisches Institut, RWTH Aachen University, Aachen, Germany
¹⁵Fakultät Physik, Technische Universität Dortmund, Dortmund, Germany
¹⁶Max-Planck-Institut für Kernphysik (MPIK), Heidelberg, Germany
¹⁷Physikalisches Institut, Ruprecht-Karls-Universität Heidelberg, Heidelberg, Germany
¹⁸School of Physics, University College Dublin, Dublin, Ireland
¹⁹INFN Sezione di Bari, Bari, Italy
²⁰INFN Sezione di Bologna, Bologna, Italy
²¹INFN Sezione di Ferrara, Ferrara, Italy
²²INFN Sezione di Firenze, Firenze, Italy
²³INFN Laboratori Nazionali di Frascati, Frascati, Italy
²⁴INFN Sezione di Genova, Genova, Italy
²⁵INFN Sezione di Milano, Milano, Italy
²⁶INFN Sezione di Milano-Bicocca, Milano, Italy
²⁷INFN Sezione di Cagliari, Monserrato, Italy
²⁸Università degli Studi di Padova, Università e INFN, Padova, Padova, Italy
²⁹INFN Sezione di Pisa, Pisa, Italy
³⁰INFN Sezione di Roma La Sapienza, Roma, Italy
³¹INFN Sezione di Roma Tor Vergata, Roma, Italy
³²Nikhef National Institute for Subatomic Physics, Amsterdam, Netherlands
³³Nikhef National Institute for Subatomic Physics and VU University Amsterdam, Amsterdam, Netherlands
³⁴AGH - University of Science and Technology, Faculty of Physics and Applied Computer Science, Kraków, Poland
³⁵Henryk Niewodniczanski Institute of Nuclear Physics Polish Academy of Sciences, Kraków, Poland
³⁶National Center for Nuclear Research (NCBJ), Warsaw, Poland
³⁷Horia Hulubei National Institute of Physics and Nuclear Engineering, Bucharest-Magurele, Romania
³⁸Affiliated with an institute covered by a cooperation agreement with CERN
³⁹ICCUB, Universitat de Barcelona, Barcelona, Spain
⁴⁰Instituto Galego de Física de Altas Enerxías (IGFAE), Universidade de Santiago de Compostela, Santiago de Compostela, Spain
⁴¹Instituto de Fisica Corpuscular, Centro Mixto Universidad de Valencia - CSIC, Valencia, Spain
⁴²European Organization for Nuclear Research (CERN), Geneva, Switzerland
⁴³Institute of Physics, Ecole Polytechnique Fédérale de Lausanne (EPFL), Lausanne, Switzerland
⁴⁴Physik-Institut, Universität Zürich, Zürich, Switzerland
⁴⁵NSC Kharkiv Institute of Physics and Technology (NSC KIPT), Kharkiv, Ukraine
⁴⁶Institute for Nuclear Research of the National Academy of Sciences (KINR), Kyiv, Ukraine
⁴⁷University of Birmingham, Birmingham, United Kingdom
⁴⁸H.H. Wills Physics Laboratory, University of Bristol, Bristol, United Kingdom
⁴⁹Cavendish Laboratory, University of Cambridge, Cambridge, United Kingdom
⁵⁰Department of Physics, University of Warwick, Coventry, United Kingdom
⁵¹STFC Rutherford Appleton Laboratory, Didcot, United Kingdom
⁵²School of Physics and Astronomy, University of Edinburgh, Edinburgh, United Kingdom
⁵³School of Physics and Astronomy, University of Glasgow, Glasgow, United Kingdom
⁵⁴Oliver Lodge Laboratory, University of Liverpool, Liverpool, United Kingdom
⁵⁵Imperial College London, London, United Kingdom
⁵⁶Department of Physics and Astronomy, University of Manchester, Manchester, United Kingdom
⁵⁷Department of Physics, University of Oxford, Oxford, United Kingdom
⁵⁸Massachusetts Institute of Technology, Cambridge, MA, United States
⁵⁹University of Cincinnati, Cincinnati, OH, United States
⁶⁰University of Maryland, College Park, MD, United States
⁶¹Los Alamos National Laboratory (LANL), Los Alamos, NM, United States
⁶²Syracuse University, Syracuse, NY, United States
⁶³School of Physics and Astronomy, Monash University, Melbourne, Australia
(associated with Institution Department of Physics, University of Warwick, Coventry, United Kingdom)
⁶⁴Pontifícia Universidade Católica do Rio de Janeiro (PUC-Rio), Rio de Janeiro, Brazil
(associated with Institution Universidade Federal do Rio de Janeiro (UFRJ), Rio de Janeiro, Brazil)
⁶⁵Physics and Micro Electronic College, Hunan University, Changsha City, China
(associated with Institution Institute of Particle Physics, Central China Normal University, Wuhan, Hubei, China)
⁶⁶Guangdong Provincial Key Laboratory of Nuclear Science, Guangdong-Hong Kong Joint Laboratory of Quantum Matter,
Institute of Quantum Matter, South China Normal University, Guangzhou, China
(associated with Institution Center for High Energy Physics, Tsinghua University, Beijing, China)

⁶⁷*Lanzhou University, Lanzhou, China**(associated with Institution Institute Of High Energy Physics (IHEP), Beijing, China)*⁶⁸*School of Physics and Technology, Wuhan University, Wuhan, China**(associated with Institution Center for High Energy Physics, Tsinghua University, Beijing, China)*⁶⁹*Departamento de Fisica, Universidad Nacional de Colombia, Bogota, Colombia**(associated with Institution LPNHE, Sorbonne Université, Paris Diderot Sorbonne Paris Cité, CNRS/IN2P3, Paris, France)*⁷⁰*Universität Bonn - Helmholtz-Institut für Strahlen und Kernphysik, Bonn, Germany**(associated with Institution Physikalisches Institut, Ruprecht-Karls-Universität Heidelberg, Heidelberg, Germany)*⁷¹*Eotvos Lorand University, Budapest, Hungary**(associated with Institution European Organization for Nuclear Research (CERN), Geneva, Switzerland)*⁷²*INFN Sezione di Perugia, Perugia, Italy**(associated with Institution INFN Sezione di Ferrara, Ferrara, Italy)*⁷³*Van Swinderen Institute, University of Groningen, Groningen, Netherlands**(associated with Institution Nikhef National Institute for Subatomic Physics, Amsterdam, Netherlands)*⁷⁴*Universiteit Maastricht, Maastricht, Netherlands**(associated with Institution Nikhef National Institute for Subatomic Physics, Amsterdam, Netherlands)*⁷⁵*Faculty of Material Engineering and Physics, Cracow, Poland**(associated with Institution Henryk Niewodniczanski Institute of Nuclear Physics Polish Academy of Sciences, Kraków, Poland)*⁷⁶*DS4DS, La Salle, Universitat Ramon Llull, Barcelona, Spain**(associated with Institution ICCUB, Universitat de Barcelona, Barcelona, Spain)*⁷⁷*Department of Physics and Astronomy, Uppsala University, Uppsala, Sweden**(associated with Institution School of Physics and Astronomy, University of Glasgow, Glasgow, United Kingdom)*⁷⁸*University of Michigan, Ann Arbor, MI, United States**(associated with Institution Syracuse University, Syracuse, NY, United States)*^aDeceased.^bAlso at Università di Firenze, Firenze, Italy.^cAlso at Scuola Normale Superiore, Pisa, Italy.^dAlso at Università di Ferrara, Ferrara, Italy.^eAlso at Università di Milano Bicocca, Milano, Italy.^fAlso at Università di Bologna, Bologna, Italy.^gAlso at Università di Genova, Genova, Italy.^hAlso at Universidad Nacional Autónoma de Honduras, Tegucigalpa, Honduras.ⁱAlso at Università di Bari, Bari, Italy.^jAlso at Università di Cagliari, Cagliari, Italy.^kAlso at Università di Perugia, Perugia, Italy.^lAlso at Università di Roma Tor Vergata, Roma, Italy.^mAlso at Universidade de Brasília, Brasília, Brazil.ⁿAlso at Hangzhou Institute for Advanced Study, UCAS, Hangzhou, China.^oAlso at Università di Siena, Siena, Italy.^pAlso at Università degli Studi di Milano, Milano, Italy.^qAlso at Central South U., Changsha, China.^rAlso at Università di Padova, Padova, Italy.^sAlso at Excellence Cluster ORIGINS, Munich, Germany.^tAlso at Università di Pisa, Pisa, Italy.^uAlso at Università della Basilicata, Potenza, Italy.^vAlso at Universidad de Alcalá, Alcalá de Henares, Spain.^wAlso at Università di Urbino, Urbino, Italy.